



## Quantum Nano-Electronics

Hervé Courtois

Institut Néel

CNRS, Université Joseph Fourier and Grenoble INP

<http://neel.cnrs.fr/spip.php?article804&lang=en>  
herve.courtois@neel.cnrs.fr

## Chapter 1: Single electronics

## Part 2: Nano-electronic devices

### 1.1 Charging

## A note on capacitance

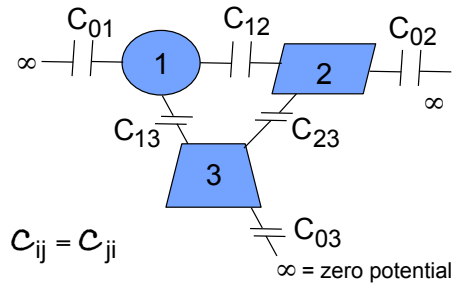
A given conductor is at a given potential. Charges and potentials are related through a capacitance matrix:

$$Q_i = \sum_j C_{ij} V_j$$

$$V_i = \sum_j C_{ij}^{-1} Q_j$$

$$C_{ij} = \begin{bmatrix} C_{01} + C_{12} + C_{13} & -C_{12} & -C_{13} \\ -C_{21} & C_{02} + C_{21} + C_{23} & -C_{23} \\ -C_{31} & -C_{32} & C_{03} + C_{31} + C_{33} \end{bmatrix}$$

Energy of the system:  $E = \frac{1}{2} \sum_{i,j} C_{ij} V_i V_j$



## Practical capacitances

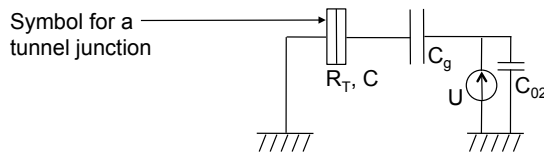
Parallel plates:  $C = \epsilon_0 \epsilon_r \frac{S}{d}$

Concentric spheres:  $C = \epsilon_0 \epsilon_r \frac{4\pi r_1 r_2}{r_2 - r_1} \approx \epsilon_0 \epsilon_r 4\pi r_1$  if  $r_1 \ll r_2$

Ex: 1 cm radius gives 0.1 pF, 1  $\mu\text{m}$  gives 0.1 fF ( $10^{-15}$ ), 10 nm gives 1 aF ( $10^{-18}$ )

## A large electrostatic energy change

Consider the electron box configuration:



The electro-static energy changes when one electron is added to the grain.

Total capacitance  $C_\Sigma = C + C_g$

$$E_c = \frac{e^2}{2C_\Sigma}$$

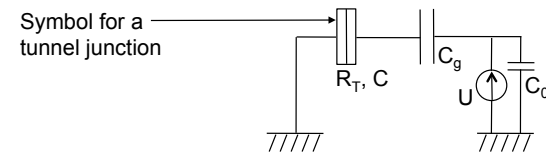
One needs  $E_c > k_B T$  in order to observe single-electron effects.

With 1 aF, one obtains  $E_c = 80 \text{ meV} > k_B T$  at ambient temperature (25 meV).

With 1 pF, one obtains  $E_c = 80 \text{ } \mu\text{eV} > k_B T$  at 0.3 K.

## A significant tunnel junction resistance

Consider the electron box configuration:



The lifetime of a charge state is the discharge time for the capacitor:

$$\tau = R_T C$$

Width of discrete levels due to charge quantization in the grain:

$$\delta = \frac{\hbar}{\tau} = \frac{\hbar}{R_T C}$$

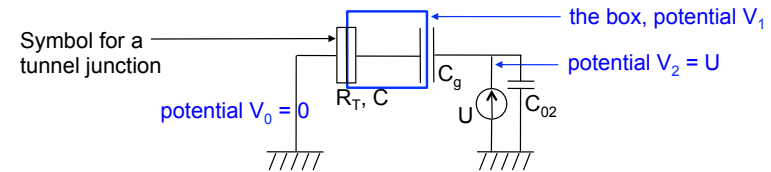
For charge discreteness to be observable, one needs:

$$\delta < E_c \approx \frac{e^2}{2C} \quad \Rightarrow \quad R_T > R_K = \frac{\hbar}{e^2} = 25.8 \text{ k}\Omega$$

## 1.2 The single electron box

## Electrostatic energy in an electron box

Consider the electron box configuration:



We define

$$C_\Sigma = C + C_g$$

$$Q = C_\Sigma V_1$$

$$Q_g = C_g U$$

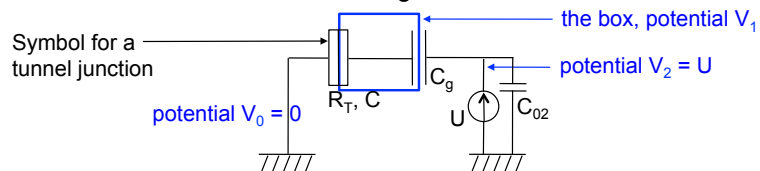
Capacitance matrix:  $\mathbf{C} = \begin{pmatrix} C + C_{02} & -C & -C_{02} \\ -C & C + C_g & -C_g \\ -C_{02} & -C_g & C_g + C_{02} \end{pmatrix}$

Electrostatic energy of the box:

$$E = \frac{1}{2} \sum_{i,j} C_{ij} V_i V_j = \frac{1}{2} \left[ (C + C_g) V_1^2 - 2C_g U V_1 + (C_g + C_{02}) U^2 \right]$$

## Electrostatic energy in an electron box

Consider the electron box configuration:



We define

$$C_\Sigma = C + C_g$$

$$Q = C_\Sigma V_1$$

$$Q_g = C_g U$$

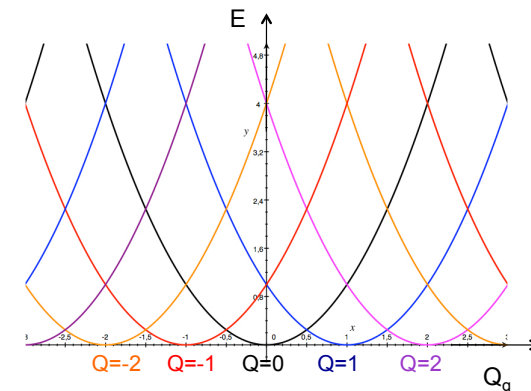
Substitute for charges, complete the square:

$$E = \frac{1}{2} \left[ (C + C_g) V_1^2 - 2C_g U V_1 + (C_g + C_{02}) U^2 \right] = \frac{1}{2} \left[ \frac{Q^2}{C_\Sigma} - \frac{2Q Q_g}{C_\Sigma} + \frac{Q_g^2}{C_\Sigma} \right] - \frac{Q_g^2}{C_\Sigma} + C_g U^2 + C_{02} U^2$$

$$E = \frac{(Q - Q_g)^2}{2C_\Sigma} + \text{terms independent of } Q \text{ related to work done by the source}$$

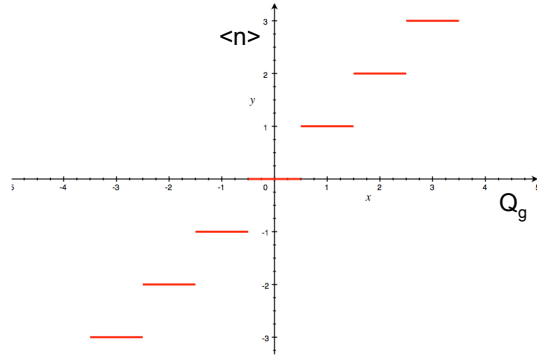
## Energy parabolas

Electrostatic energy as a function of gate charge for various  $Q = -ne$   
Gate charge is a continuous variable,  $Q$  a quantized one.



## Charge in the fundamental state

Charge state defined by the minimum energy: the Coulomb staircase.  
Island charge is a step function of the gate voltage.  
Valid at  $T = 0$ .



## Effect of temperature

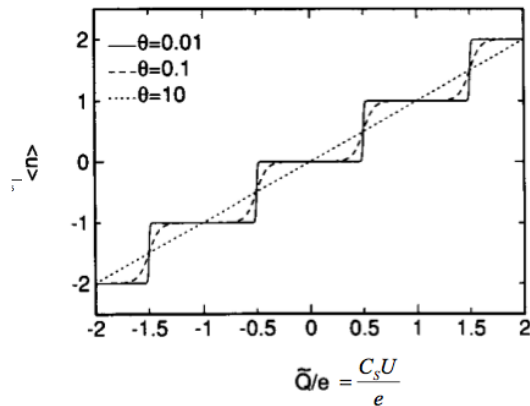
At thermal equilibrium, Boltzmann distribution:

$$\langle n \rangle = \frac{\sum_{n=-\infty}^{\infty} n \exp\left(\frac{-E(n)}{k_B T}\right)}{\sum_{n=-\infty}^{\infty} \exp\left(\frac{-E(n)}{k_B T}\right)}$$

depends on the parameter  $\frac{k_B T}{e^2 / 2C_\Sigma}$

## Charge in the fundamental state

The staircase is smeared by temperature.



$$\theta = \frac{kT}{e^2 / C_\Sigma}$$

## 1.4 Practical implementation



## Low temperatures

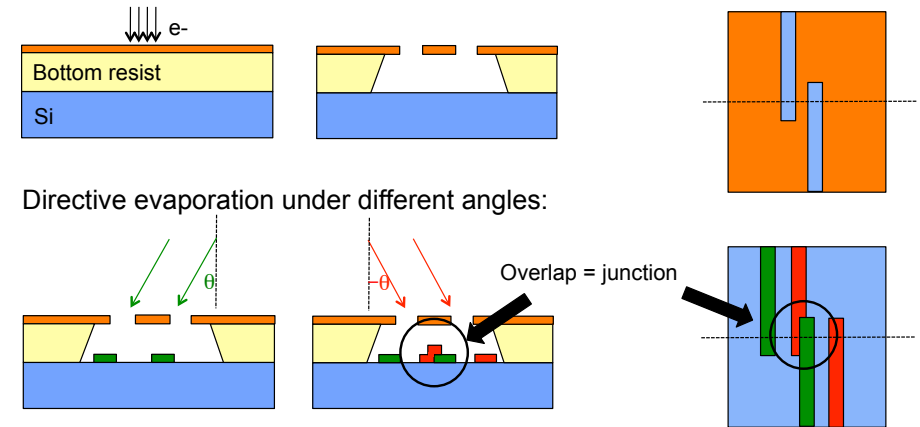
Temperature of 4.2 K reached with a liquid He bath in equilibrium with its vapor, 1 K with pumping, 0.25 K same thing with pure He3.

Temperature down to about 0.02 K = 20 mK with mixture of He3 and He4: dilution refrigerator.



## Angle evaporation technique

Bilayer of resist with the bottom layer more sensitive, bridges can be realized.

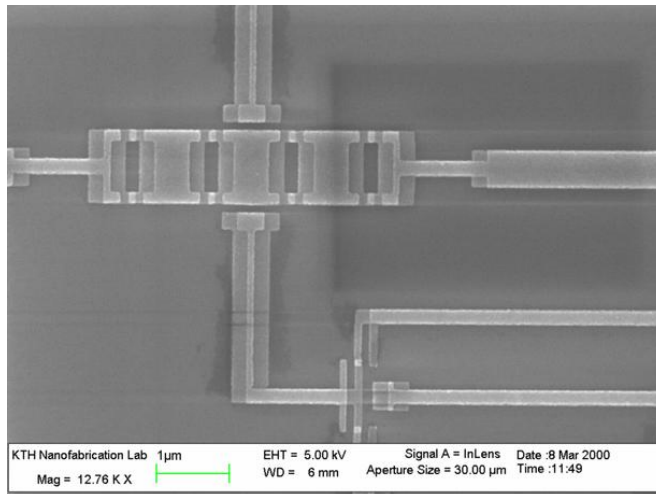
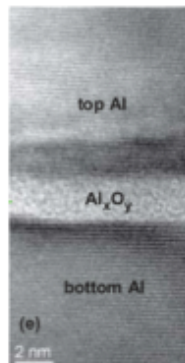


An oxidation can be realized between the two depositions: tunnel junction

## A typical sample

Al oxide preferred: reliable, reproducible, despite amorphous nature.

Complex devices can be build.

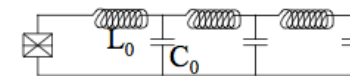


## A fact of nature

Device connected through rather long wires: 1-2 meters if low T.  
At high frequency, wires must be regarded as transmission lines.

Impedance close to the vacuum characteristic impedance  $Z_0$ .

$$Z_0 = \frac{1}{\epsilon_0 c} \approx 376 \, \Omega$$



Fact of Nature: free space impedance much lower than Quantum resistance.

$$\frac{Z_L}{R_K} = \frac{e^2}{2\pi\hbar c \epsilon_0} \approx \frac{\alpha}{\pi}$$

Fine structure constant:  $\alpha = \frac{1}{137.036}$

The free space effectively shunts the tunnel junction.

Need to have a highly resistive element close to the device: a resistor or another tunnel junction. Very close: distance less than photon wavelength.

## A single electron box

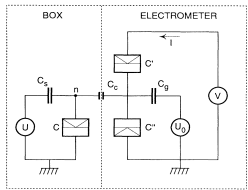


FIG. 1. Circuit diagram of the experiment. The rectangular symbols represent SN tunnel junctions. The V-shaped marks denote superconducting electrodes. The symbol  $n$  denotes the number of electrons in the island of the box (marked by a full dot). The variations of its average  $\bar{n}$  with the voltage  $U$  are detected by monitoring the current  $I$  through the SNS electrometer which is coupled to the box through the capacitor  $C_g$ . The bias voltage  $V$  and the gate voltage  $U_g$  set the working point of the electrometer.

P. Lafarge, P. Joyez, D. Estève, C. Urbina, and M. H. Devoret, PRL 70, 994 (1993).  
Electrometer = SET (see what follows)

With a superconducting island, extra energy  $\Delta$  for odd number of e-.

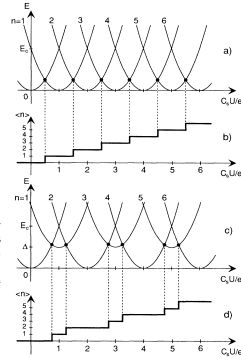


FIG. 2. Ground-state energy of the box in the (a) normal and (c) superconducting states as a function of the polarization  $C_g U/e$ , for several values of the excess number  $n$  of electrons in the island.  $E_n$  is the electrostatic energy of one excess electron on the island for  $U=0$ . In an ideal superconductor, the minimum energy for odd  $n$  is  $\Delta$  above the minimum energy for even  $n$ . The dots correspond to level crossings where single electron tunneling is possible. Equilibrium value  $\bar{n}$  vs  $C_g U/e$  is shown in the (b) normal and (d) superconducting states, at  $T=0$ .

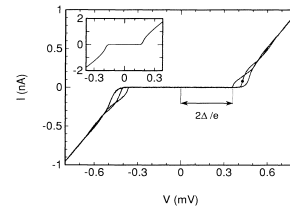


FIG. 3.  $I(V)$  curves for the SNS electrometer at  $T=25$  mK, and zero magnetic field, for three values of the gate voltage  $U_g$  corresponding to maximum, intermediate, and minimum gap. The minimum gap corresponds to the bare superconducting gap  $2\Delta$  of two NS junctions in series. The dot indicates the optimal bias point for maximum sensitivity. Inset:  $I(V)$  curve for a single SN junction under the same conditions.

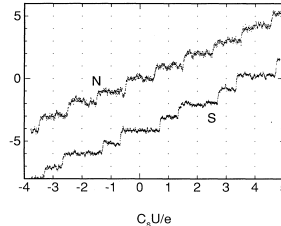


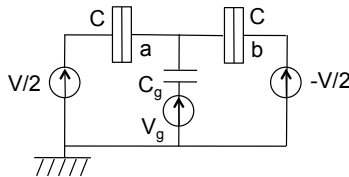
FIG. 4. Variations of the average value  $\bar{n}$  of the number of extra electrons in the box as a function of the polarization  $C_g U/e$ , at  $T=25$  mK. Trace N: normal island. Trace S: superconducting island. For clarity, trace S has been offset vertically by 4 units.

## 1.4 The SET and the turnstile



## The Single Electron Transistor (SET)

Consider the configuration with two tunnel junctions:



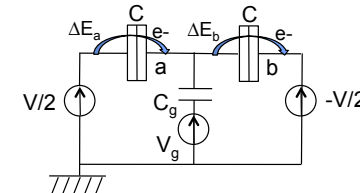
The electro-static energy is identical to the box case,  $Q = -ne$ :

$$E_c(n) = \frac{(-ne - Q_g)^2}{2C_\Sigma} \quad \text{where } C_\Sigma = 2C + C_g$$

The current through the turnstile depends on the gate voltage:  
Single Electron Transistor = SET  
and also on temperature.

## The Single Electron Transistor (SET)

Consider the configuration with two tunnel junctions:



Opposite transitions:  $-\Delta E_{a,b}$

Energy changes when one electron tunnels from left to central island:  $n-1 \rightarrow n$ , work done by the source  $eV/2$  taken into account:

$$\Delta E_a = \frac{eV}{2} + E_c(n) - E_c(n-1) = \frac{eV}{2} + \frac{e[C_g V_g + (n-1/2)e]}{C_\Sigma}$$

Similar expression for tunneling from center to right:  $n \rightarrow n-1$ .

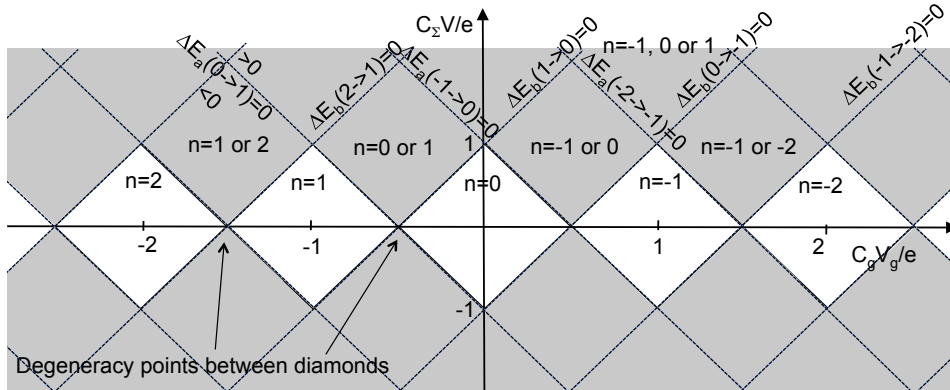
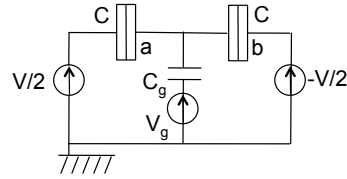
$$\Delta E_b = \frac{eV}{2} + E_c(n-1) - E_c(n) = \frac{eV}{2} - \frac{e[C_g V_g + (n-1/2)e]}{C_\Sigma}$$

## The stability diagram

$$\Delta E_a = 0 \quad \text{if } C_\Sigma V/2 = -C_g V_g - n + 1/2$$

$\Delta E_{a,b} = 0$  define lines in a  $C_g V_g/e$  ;  $C_\Sigma V/e$  plane: Coulomb diamonds limits.

A given tunneling process changes direction when one crosses the related line.

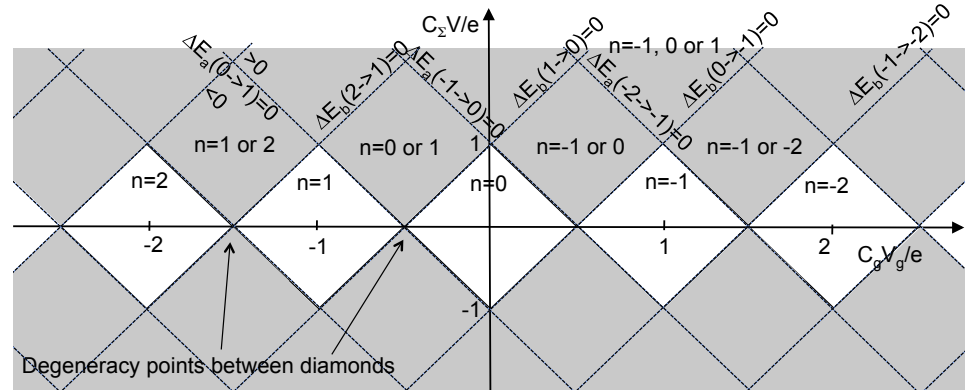
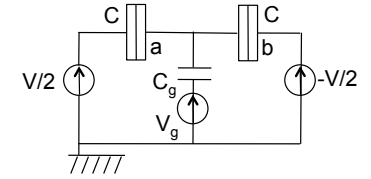


## The stability diagram

Different zones:

well-defined charge state in central diamond: no current.

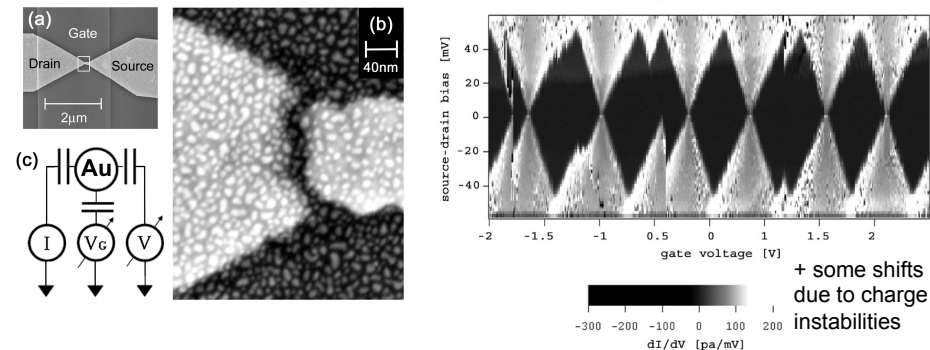
bistable state in next line: current appears.



## Coulomb diamonds

A SET or turnstile can be formed through a nano-particle bridging a gap formed by electro-migration.

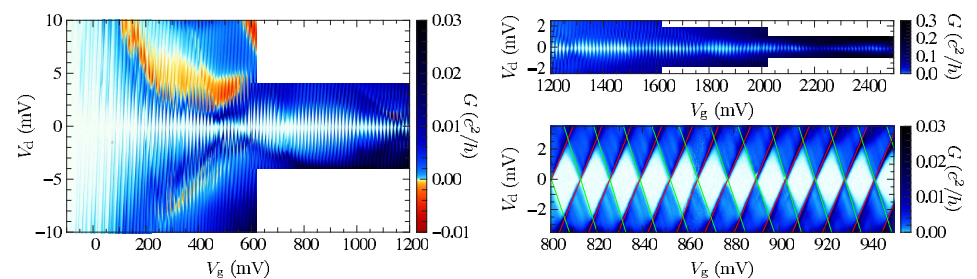
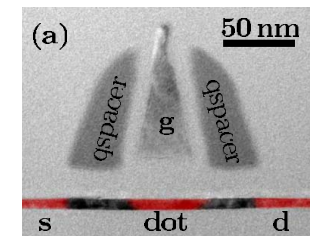
Differential conductance plotted in a  $V$  ;  $V_g$  plane.  $T = 4.2$  K:



K. I. Bolotin, D. C. Ralph et al, Appl. Phys. Lett. 84, 3154 (2004).

## Coulomb diamonds

A MOS-FET transistor of nanometric scale,  
A quantum dot defined by the gate between source and drain.

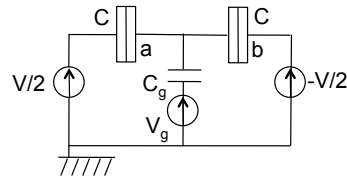
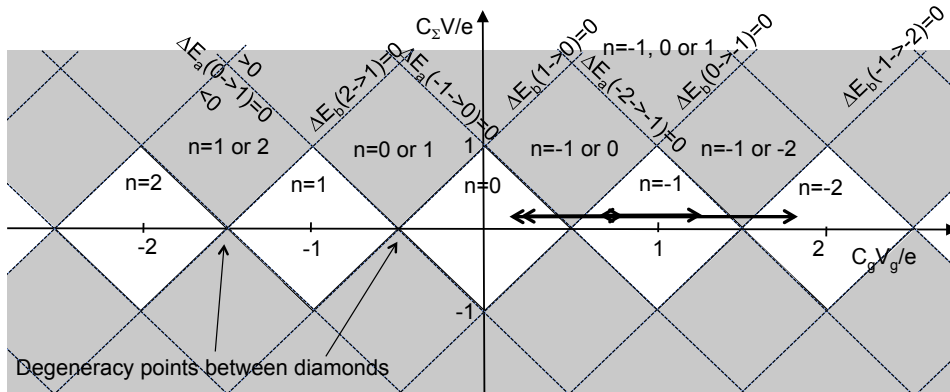


M. Hofheinz, X. Jehl, M. Sanquer, G. Molas, M. Vinet, and S. Deleonibus, Phys. Rev. B 75, 235301 (2007).

## The stability diagram

The same configuration with a rf bias at the gate.

Fast gate cycling through bistable region shuttles electrons through the device.



## The turnstile as a current source

Practical example of a turnstile: a I-V shows Coulomb blockade.

Limited accuracy: current not limited when crossing degeneracy point.

L. J. Geerligs et al, PRL 64, 2691 (1994).

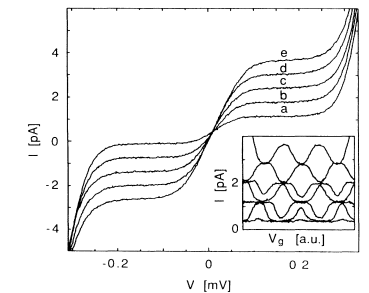
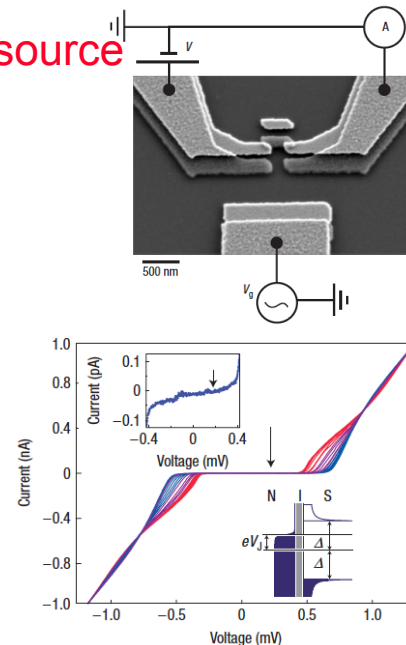


FIG. 2. Current-voltage characteristics without ac gate voltage (dotted curve) and with applied ac gate voltage at frequencies  $f$  from 4 to 20 MHz in 4-MHz steps (a-e). Current plateaus are seen at  $I = ef$ . Inset: Current vs dc-gate-voltage characteristics for  $f = 5$  MHz. The curves tend to be confined between levels at  $I = nef$  and  $(n+1)ef$ , with  $n$  an integer. The bias voltage was fixed at 0.15 mV. For the bottom curve, which is nearly flat, the ac-gate-voltage amplitude is 0. For the other curves the calculated ac gate-voltage amplitude increases from  $0.60e/C$  for the lowest one to  $3.4e/C$  for the upper one, where  $e/C = 0.30$  mV.

## The turnstile as a current source

Practical example of a SINIS turnstile: a I-V shows Coulomb blockade. Gate dependence of the current.

J. P. Pekola et al, Nature Phys. 4, 120 (2008).

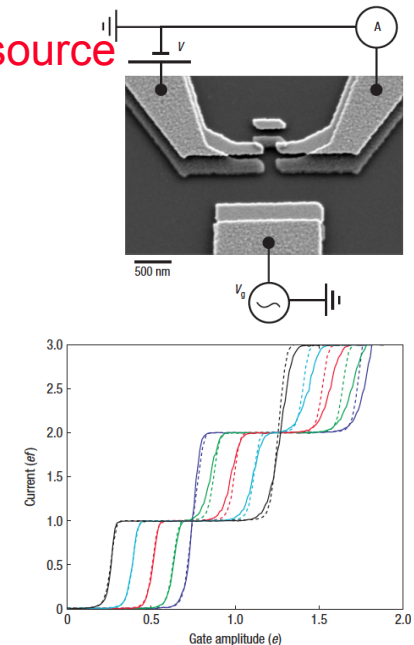


## The turnstile as a current source

Practical example of a SINIS turnstile: a rf signal applied to the gate.

Plateaus at  $I = n.ef$ : possible current standard.

Depending on the mean gate bias value, plateaus of different width behavior.

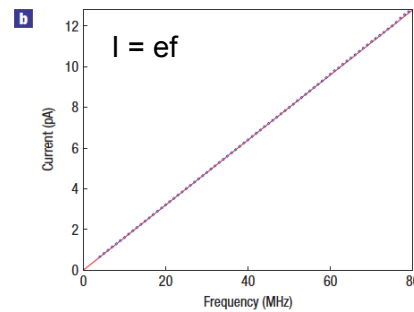
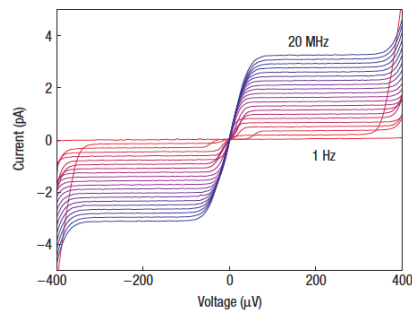
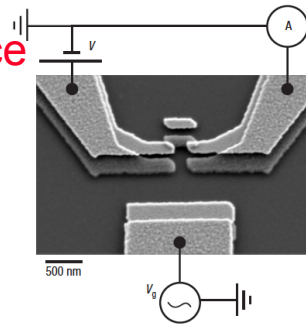


## The turnstile as a current source

Practical example of a SINIS turnstile: a rf signal applied to the gate.

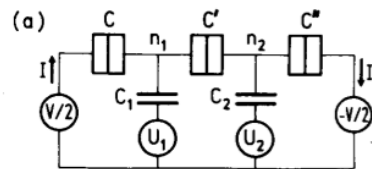
$$I = ef$$

Bias sign changes: current changes sign



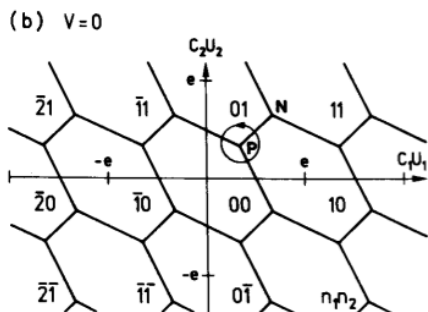
## 1.5 Pumping electrons

## The electron pump



Three junctions.

Stability diagram: numbers inside each cell of the honeycomb give the charge configuration that has the minimum energy.



Transition rate to a new configuration is given by usual rate equation.

Creating a circular cycle with gate voltages allows one to move one charge with each cycle.

## A 7-junction pump

Co-tunneling through two junctions at a time dominates errors in a usual current pump. Error down to 15 ppb with 7-junction pump.

M. W. Keller et al, APL 69, 1804 (1996).

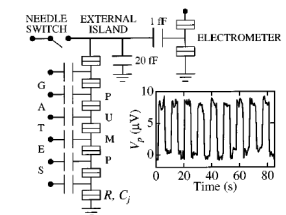


FIG. 2. Schematic of the circuit used to study the pump. All components except the needle switch were fabricated on a single chip. The entire circuit was placed in a copper box attached to the mixing chamber of a dilution refrigerator. Coaxial lines entering the box were heavily attenuated (gates) or filtered (others). The plot shows  $V_p$  vs time when pumping  $\pm e$  with a wait time of 4.5 s between electrons.

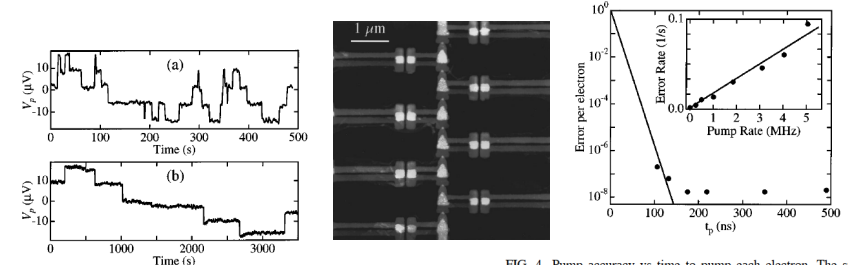


FIG. 3. Pump voltage vs time showing individual error events. (a) Pumping  $\pm e$  at 5.05 MHz, average error per electron=15 ppb. (b) Hold mode, average hold time  $\sim 600$  S.  $T_{mc}=35$  mK for both plots.

FIG. 4. Pump accuracy vs time to pump each electron. The speed of the electronics used to create the gate pulses limited the experiment to  $t_p \geq 100$  ns. The line is Eq. (1) with  $a=0.021$ . Inset: error rate vs overall pump rate  $1/(t_p + t_w)$  for  $t_p=175$  ns. The line represents a constant error per electron of 16 ppb.  $T_{mc}=35$  mK,  $V_p \approx 0$  for both plots.



## Chapter 2: Josephson junctions

## 2.1 Fundamentals on Josephson devices

### The superconducting condensate

Cooper pairs are condensed in a single macroscopic quantum state:

$$\Psi(\mathbf{x}) = |\Psi(\mathbf{x})| e^{i\varphi(\mathbf{x})}$$

The wavefunction amplitude describes the Cooper density.

The phase is related to the superconducting current:

$$\vec{j} = -\frac{e}{m} [2e\vec{A} + \hbar \vec{\nabla} \varphi] |\Psi(\mathbf{x})|^2$$

It gives rise to flux quantization (vortices) and interference effects.

### The Josephson effect

Consider a weak link between two superconductors:

tunnel junction, constriction, normal metal bridge, molecule ...

A supercurrent  $I_s$  can flow:

$$I_s = I_c \sin(\varphi_1 - \varphi_2)$$

which is directly to the difference between the superconducting phases.

If voltage is non-zero:

$$\frac{d\varphi}{dt} = \frac{2eV}{\hbar}$$

Two Josephson relations (1960).

## The critical current

depends on physics at the micro/nanoscale.

In a tunnel junction, Ambegaokar-Baratoff relation:

$$R_n I_c = \frac{\pi \Delta(T)}{2e} \tanh \left[ \frac{\Delta(T)}{2k_B T} \right]$$

In a short weak link (constriction made of the same superconductor):

$$R_n I_c \approx \Delta/e$$

In a long normal metal of length  $L$  and diffusion coefficient  $D$ , at  $T = 0$ :

$$e R_n I_c \approx \frac{\hbar D}{L^2} \quad \text{which is the Thouless energy}$$

## The Josephson energy

Work given by the generator during a time  $\Delta t$  to obtain the current:

$$W = \int_0^{\Delta t} V(t) I(t) dt = \frac{\hbar I_c}{2e} \int_0^{\theta} \sin \theta' d\theta' = \frac{\hbar I_c}{2e} [1 - \cos \theta]$$

This is also the potential energy of the junction:

$$E = E_J [1 - \cos \theta]$$

We have defined the Josephson energy:

$$E_J = \frac{\hbar I_c}{2e}$$

If thermal smearing  $kT$  is above  $E_J$ , then the phase value is not well defined and the JJ does not operate properly. This gives :

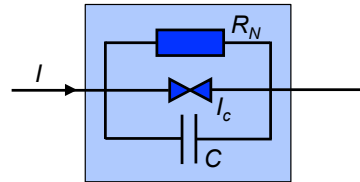
$$I_c \gg 0.04 \mu A / K$$

## At non-zero voltage: the R(C)SJ model

Resistively and Capacitively Shunted Junction:

$$I = \frac{V}{R_N} + C \frac{dV}{dt} + I_c \sin \varphi$$

$$\text{and: } \frac{d\varphi}{dt} = \frac{2eV}{\hbar}$$



$$\text{Combining the two gives: } \frac{d^2 \varphi}{d\tau^2} + Q^{-1} \frac{d\varphi}{d\tau} + \sin \varphi = \frac{I}{I_c}$$

$$\text{with } \omega_p = \sqrt{\frac{2eI_c}{\hbar C}}, \tau = \omega_p t, \quad \boxed{Q = \omega_p R_N C} \quad (\text{quality factor})$$

## The R(C)SJ model

$$\text{Equation of evolution: } \frac{d^2 \varphi}{d\tau^2} + Q^{-1} \frac{d\varphi}{d\tau} + \sin \varphi = \frac{I}{I_c}$$

equivalent to eq. of motion for a massive particle in a tilted wash-board potential:

$$U(\varphi) = E_J (1 - \cos \varphi) - \frac{\hbar I}{2e}$$

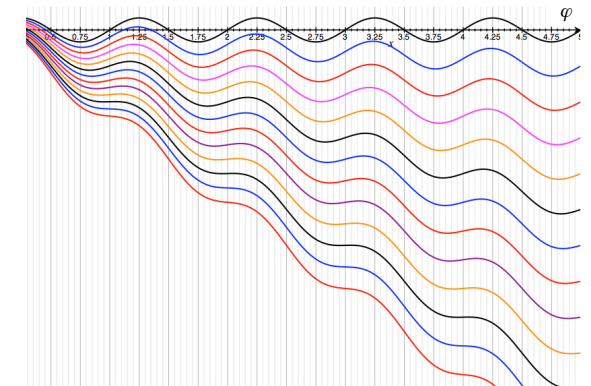
Position =  $\varphi$

Mass =  $C$

Velocity = voltage

Potential period =  $2\pi$

Potential slope = bias current



## The R(C)SJ model

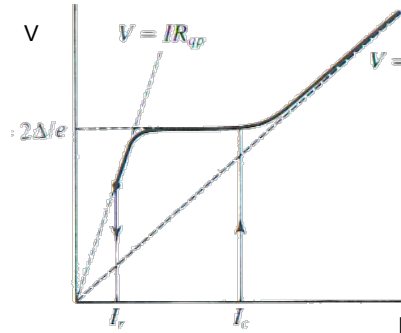
$Q > 1$  (large C, tunnel junctions): full RCSJ model.

Underdamped regime:

after escape, kinetic energy is conserved, hysteretic I(V).

In the sub-gap regime  $eV < 2\Delta$  of a tunnel junction, the shunt resistance is exponentially increased:

$$R_{qp} = R_N \exp\left(\frac{\Delta}{k_B T}\right)$$



M. Tinkham's book

## Retrapping current (1)

If  $Q \gg 1$ , one neglects damping in the evolution eq.:  $I = I_c \sin \varphi + C \frac{\phi_0}{2\pi} \frac{d^2 \varphi}{dt^2}$

Let's calculate the energy:  $E = \frac{\phi_0}{2\pi} \int_0^\varphi I d\varphi' = \frac{\phi_0}{2\pi} \int_0^\varphi \left( I_c \sin \varphi' + C \frac{\phi_0}{2\pi} \frac{d^2 \varphi'}{dt^2} \right) d\varphi'$

$$E = E_J \left[ (1 - \cos \varphi) + \frac{1}{\omega_p^2} \int_0^t \frac{d^2 \varphi'}{dt'^2} \frac{d\varphi'}{dt'} dt' \right] = E_J \left[ \underbrace{(1 - \cos \varphi)}_{\text{Josephson}} + \underbrace{\frac{1}{2\omega_p^2} \left( \frac{d\varphi}{dt} \right)^2}_{\text{kinetic}} \right]$$

We can thus write:  $\frac{d\varphi}{dt} = \left[ 2\omega_p^2 \left( \frac{E}{E_J} - 1 + \cos \varphi \right) \right]^{1/2}$

Dissipated power in one cycle is:  $W_{\text{diss}} = \int_0^T \frac{V^2}{R} dt = \frac{1}{R} \left( \frac{\hbar}{2e} \right)^2 \int_0^T \frac{d\varphi}{dt} \frac{d\varphi}{dt} dt = \frac{1}{R} \left( \frac{\hbar}{2e} \right)^2 \int_0^{2\pi} \frac{d\varphi}{dt} d\varphi$

## Retrapping current (2)

Using the expression of the phase time derivative:

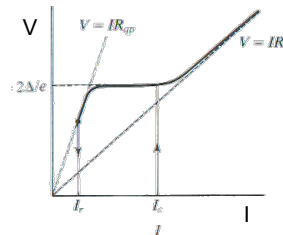
$$W_{\text{diss}} = \frac{\omega_p}{R} \left( \frac{\hbar}{2e} \right)^2 \int_0^{2\pi} 2 \left( \frac{E}{E_J} - 1 + \cos \varphi \right)^{1/2} d\varphi$$

$$\text{Just before retrapping } \frac{d\varphi}{dt} = \left[ 2\omega_p^2 \left( \frac{E}{E_J} - 1 + \cos \varphi \right) \right]^{1/2} = 0$$

This occurs (first) at  $\varphi = \pi$ , then  $E = 2 E_J$

Over a cycle dissipated power = energy gain, i.e.  $W_{\text{diss}} = \Delta E_J$ .

$$W_{\text{diss}} = \frac{\omega_p}{R} \left( \frac{\hbar}{2e} \right)^2 4 = \frac{\hbar I_r}{2e} 2\pi \quad \Rightarrow \quad I_r = \frac{\omega_p}{R} \frac{\hbar}{2e} \frac{4}{2\pi} = \frac{4}{\pi Q} I_c$$



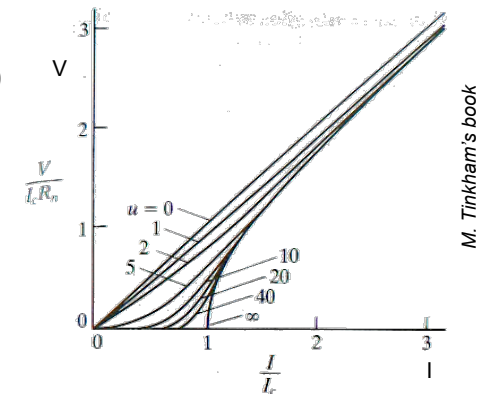
## The R(C)SJ model

$Q < 1$  (small C, lateral junctions): RSJ model.

Overdamped regime: zero mass, non-hysteretic I(V) predicted.

$$V = R_N \sqrt{I^2 - I_c^2}$$

Smeared with temperature.



M. Tinkham's book



## IV in the RSJ model

The voltage is not stationary, but oscillates at high frequency. If  $T$  is the period of oscillation of the phase:

$$\frac{d\theta}{dt} = \frac{2eV}{\hbar} \quad \int_0^{2\pi} d\theta = \frac{2e}{\hbar} \int_0^T V(t) dt = \frac{2e}{\hbar} \langle V \rangle T \quad \frac{1}{T} = \frac{2e}{\hbar} \langle V \rangle$$

We neglect the capacitance term:  $V = R_N(I - I_c \sin \theta)$

We can write:  $dt = \frac{\hbar}{2eR_N} \left( \frac{1}{I - I_c \sin \theta} \right) d\theta$

integrate it:  $\int_0^T dt = T = \frac{\hbar}{2eR_N} \int_0^{2\pi} \frac{d\theta}{I - I_c \sin \theta}$

and use the expression of  $\langle V \rangle$  to obtain:

$$\frac{1}{\langle V \rangle} = \frac{1}{2\pi R_N} \int_0^{2\pi} \frac{d\theta}{I - I_c \sin \theta} = \frac{1}{2\pi R_N} \frac{2\pi}{\sqrt{I^2 - I_c^2}} = \frac{1}{R_N \sqrt{I^2 - I_c^2}} \quad \langle V \rangle = R_N \sqrt{I^2 - I_c^2}$$

## Time dependence in the RSJ model

We integrate over time from 0 to  $t$ :  $\int_0^t dt = t = \frac{\hbar}{2eR_N} \int_0^\varphi \frac{d\theta}{I - I_c \sin \theta}$

Using:  $\int \frac{1}{I - I_c \sin \theta} d\theta = \frac{2}{\sqrt{I^2 - I_c^2}} \arctan \left( \frac{I \tan\left(\frac{\theta}{2}\right) - I_c}{\sqrt{I^2 - I_c^2}} \right)$

We write:  $t = \frac{\hbar}{2eR_N} \frac{2}{\sqrt{I^2 - I_c^2}} \arctan \left( \frac{I \tan\left(\frac{\varphi}{2}\right) - I_c}{\sqrt{I^2 - I_c^2}} \right) = \frac{2}{\omega_J} \arctan \left( \frac{I \tan\left(\frac{\varphi}{2}\right) - I_c}{\sqrt{I^2 - I_c^2}} \right)$

$$\sqrt{I^2 - I_c^2} \tan\left(\frac{\omega_J t}{2}\right) = I \tan\frac{\varphi}{2} - I_c \quad \omega_J = \frac{2e\langle V \rangle}{\hbar}$$

## IV in the RSJ model

Integral tables give:  $\int \frac{1}{I - I_c \sin \theta} d\theta = \frac{2}{\sqrt{I^2 - I_c^2}} \arctan \left( \frac{I \tan\left(\frac{\theta}{2}\right) - I_c}{\sqrt{I^2 - I_c^2}} \right)$   
 $= 0$  for  $\theta = 0$  and  $2\pi$ .

By taking distinct values of the arctan for the same argument, the integral is  $\pi$ :

$$\arctan \left( \frac{-I_c}{\sqrt{I^2 - I_c^2}} \right)^{\theta=2\pi} - \arctan \left( \frac{-I_c}{\sqrt{I^2 - I_c^2}} \right)^{\theta=0} = \pi$$

Then:  $\frac{1}{\langle V \rangle} = \frac{1}{2\pi R_N} \int_0^{2\pi} \frac{d\theta}{I - I_c \sin \theta} = \frac{1}{2\pi R_N} \frac{2}{\sqrt{I^2 - I_c^2}} \pi = \frac{1}{R_N \sqrt{I^2 - I_c^2}}$   
 $\langle V \rangle = R_N \sqrt{I^2 - I_c^2}$

## Time dependence in the RSJ model

We differentiate / time:  $\sqrt{I^2 - I_c^2} \frac{1}{\cos^2\left(\frac{\omega_J t}{2}\right)} \frac{\omega_J}{2} = \frac{I}{2} \frac{1}{\cos^2\left(\frac{\varphi}{2}\right)} \frac{2eV}{\hbar}$

which gives:  $V = R_N \frac{I^2 - I_c^2}{I} \frac{\cos^2\left(\frac{\varphi}{2}\right)}{\cos^2\left(\frac{\omega_J t}{2}\right)}$

We write:

$$\cos^2 \frac{\varphi}{2} = \left\{ 1 + \left[ \frac{\sqrt{I^2 - I_c^2}}{I} \tan \frac{\omega_J t}{2} + \frac{I_c}{I} \right]^2 \right\}^{-1}$$

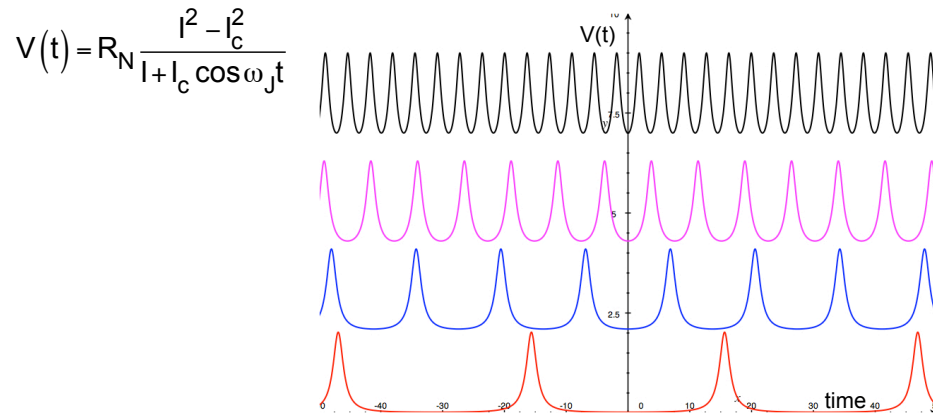
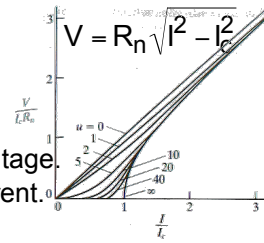
$$\frac{\cos^2 \frac{\varphi}{2}}{\cos^2 \frac{\omega_J t}{2}} = \left\{ 1 + \frac{I_c}{I} \left[ \frac{\sqrt{I^2 - I_c^2}}{I} \sin \omega_J t + \frac{I_c}{I} \cos \omega_J t \right]^2 \right\}^{-1} = \left\{ 1 + \frac{I_c}{I} \cos \omega_J t' \right\}^{-1}$$

New time reference

We need to remove  $\varphi$   
 $\tan^2 = \frac{1}{\cos^2} - 1$

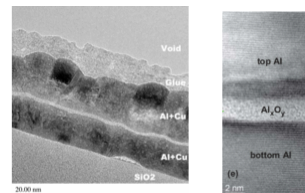
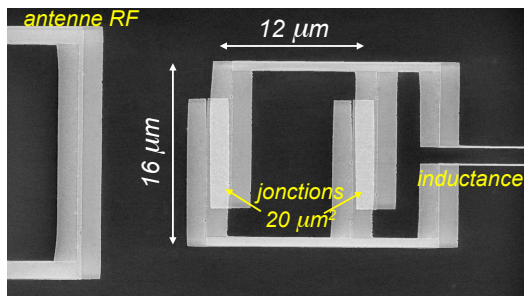
## The RSJ model

The phase oscillates in time non-sinusoidally at low voltage.  
At small (non-zero)  $V$ , part of the current is a supercurrent.



## Tunnel junctions ...

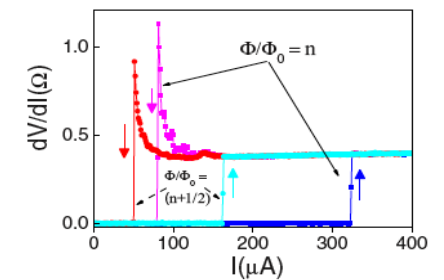
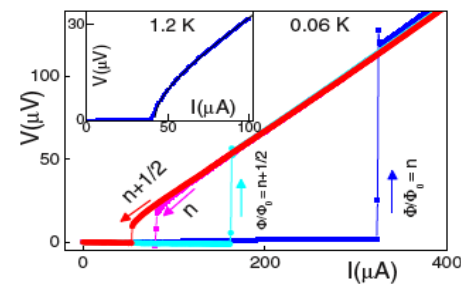
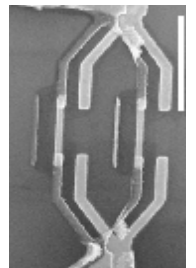
Al oxide preferred: reliable, reproducible, despite amorphous nature.  
Complex devices can be build.



## 2.2 Practical Josephson junctions

### ... normal metals ...

Routinely observed when critical current is large.  
Possibly thermal origin,  
hypothesis of an intrinsic effect (effective capacitance).

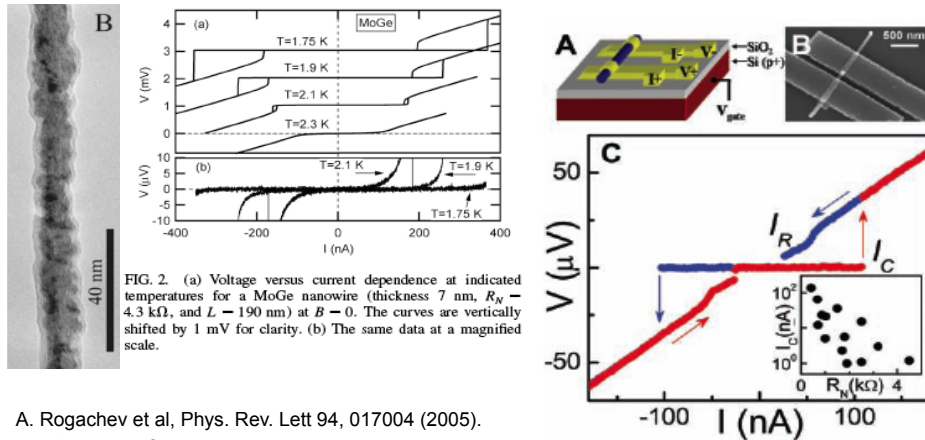


L. Angers et al, PRB 77, 165408 (2008).

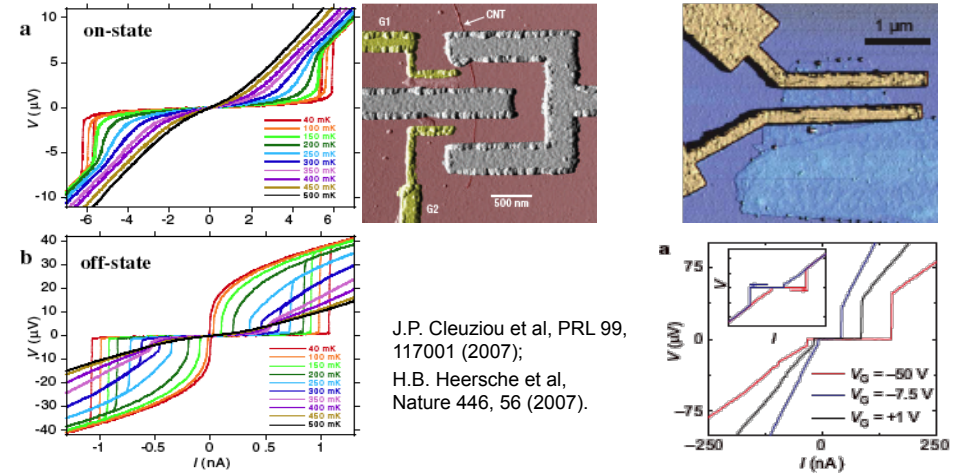
... nanowires, ...

... carbon-based devices, ...

From Nb nanowires templated by a CNT to InAs semiconducting nanowires ...



From carbon nanotubes to graphene ...



## 2.3 SQUIDS

## Superconducting Quantum Interference Device (SQUID)

SQUID = two Josephson junctions in parallel.

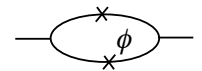
Let's integrate  $\vec{j} = -\frac{e}{m} [2e\vec{A} + \hbar \vec{\nabla} \varphi] |\Psi(x)|^2$  along the loop.

Pair density constant, current density neglected:

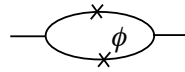
$$0 = \hbar(\varphi_1 - \varphi_2) + 2eBS - \hbar(\varphi'_1 - \varphi'_2)$$

The phase jump at the two junctions differs by  $2eBS/\hbar = 2\pi\Phi/\Phi_0$

$$\varphi'_1 - \varphi'_2 = \varphi_1 - \varphi_2 + 2\pi A\varphi$$



## Superconducting Quantum Interference Device (SQUID)



The two supercurrents add coherently.

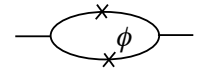
Flux through the loop adds a potential vector term  $2\pi\Phi/\Phi_0$

If loop self-inductance can be neglected:

$$I_s = I_{c0} \sin(\varphi_1 - \varphi_2) + I_{c0} \sin\left(\varphi_1 - \varphi_2 + 2\pi \frac{\Phi}{\Phi_0}\right)$$

where  $\Phi_0 = h/2e = 2.05 \cdot 10^{-15} \text{ T}\cdot\text{m}^2 = 2.05 \text{ mT}\cdot\mu\text{m}^2$   
is the superconducting flux quantum.

## Superconducting Quantum Interference Device (SQUID)

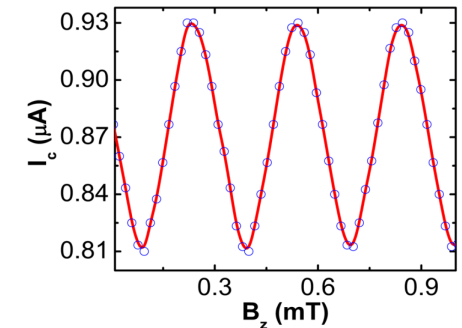


One obtains:  $I_s = 2I_{c0} \sin(\varphi_1 - \varphi_2) \cos\left(\pi \frac{\Phi}{\Phi_0}\right)$

$$I_c = 2I_{c0} \left| \cos\left(\pi \frac{\Phi}{\Phi_0}\right) \right|$$

Critical current is modulated by the magnetic flux through the loop. Even if there is no flux through the two wires.

Analogous to Young's slit experiment in optics.



S. Mandal et al, ACS Nano 5, 7144 (2011).

## Example of SQUID application

Critical current measurements = access to the flux through the loop.

High sensitivity.

Magneto-encephalography: array of SQUIDs.

Magnetic field signals of about  $10^{-15} \text{ T}$ .

Extreme field shielding necessary.



## 2.3 Shapiro steps

## The Josephson frequency

Consider a Josephson junction biased at a fixed voltage:

$$\frac{d\Theta}{dt} = \frac{2eV}{\hbar}$$

Then the phase evolves with time:

$$\Theta(t) = \Theta(0) + \left( \frac{2eV}{\hbar} \right) t$$

which leads to a time-dependent current

$$I = I_c \sin [\Theta(t)] = I_c \sin \left[ \left( \frac{2eV}{\hbar} \right) t + \Theta(0) \right]$$

at the Josephson frequency:

$$\omega_J = \frac{2eV}{\hbar} = 3.10^9 \text{ Hz}/\mu\text{V}$$

## Shapiro steps

Apply a rf signal to a Josephson junction:  $V = V_0 + v \cos(\omega_0 t + \varphi)$

The response is:  $\Theta(t) = \frac{2e}{\hbar} V_0 t + \frac{2e}{\hbar \omega_0} v \sin[\omega_0 t + \varphi] + \Theta(0)$

The current can be written as:

$$I = I_c \sum_{n=-\infty}^{\infty} (-1)^n j_n \left( \frac{2e}{\hbar \omega_0} v \right) \sin \left[ \left( \frac{2e}{\hbar} V_0 \pm n \omega_0 \right) t + \delta_n \right]$$

$j_n$  is the Bessel function of order  $n$ , and  $\delta_n = \pm n\varphi + \Theta(0)$

The sine components average to zero, except for:  $V_0 = V_n = n \frac{\hbar \omega_0}{2e}$  ( $n$  integer)

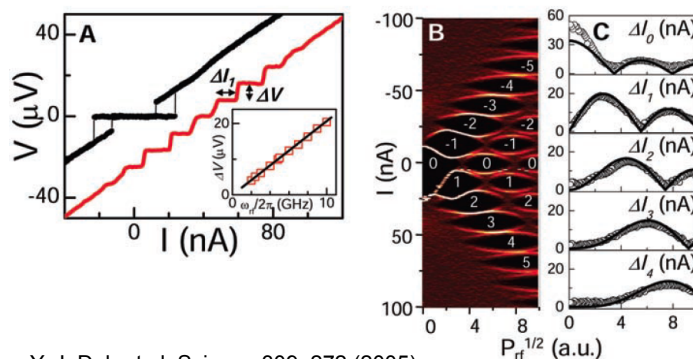
The  $n$  term  $I_n = I_c j_n \left( \frac{2e}{\hbar \omega_0} v \right) \sin \delta_n$  can take any value below:

$$I_c j_n \left( \frac{2e}{\hbar \omega_0} v \right) \quad \text{in absolute value.}$$

## Shapiro steps

Steps in the I-V characteristics at well-defined voltages.

Widths of the steps follow the Bessel functions: non-monotonous evolution.



Y. J. Doh et al, Science 309, 272 (2005).

## The Volt standard

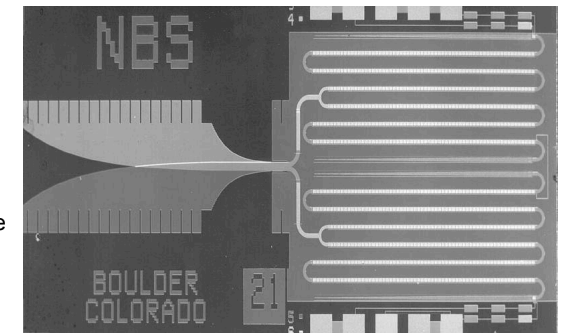
The Josephson effect relates a voltage and a time.

Combined with Cesium 133 atomic clock reference,

It provides a standard for the Volt, with the exact constant value:

$$K_{J-90} = 2e/h = 483\,597.9 \text{ GHz/V}$$

One-volt voltage standard based on an array of 3020 JJ. Microwave field fed into the fin guide structure on the left generates a voltage across the 4 chains of JJ on the right. Source: NIST.



## Chapter 3: Superconducting quantum bits

### 3.1 Charge-phase uncertainty relation

#### At non-zero voltage: the RCSJ model

Energy in the system (resistance neglected):

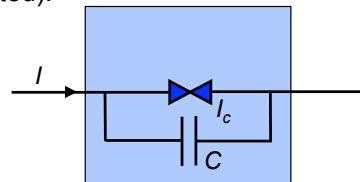
$$E = \frac{Q^2}{2C} + E_J(1 - \cos \varphi) \approx \frac{Q^2}{2C} + E_J \varphi^2$$

To be compared with

$$E = \frac{1}{2} k q^2 + \frac{p^2}{2m}$$

Heisenberg uncertainty relation  $\Delta p \Delta q \approx \hbar$   
can be translated into  $\Delta Q \Delta \varphi \approx e$

Unit is charge,  $e$  is the only charge quanta.



#### Different regimes

$$\Delta Q \Delta \varphi \approx e$$

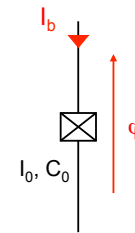
Two “classical” regimes plus a quantum one:

- Phase well defined, charge not well defined: usual Josephson effect.
- Charge well-defined, phase not defined: Coulomb blockade, single electron physics.
- Intermediate quantum regime, where Heisenberg relation operates fully.

Quantum bits can be implemented in various cases.

## 3.2 MQT

## A quantum anharmonic oscillator

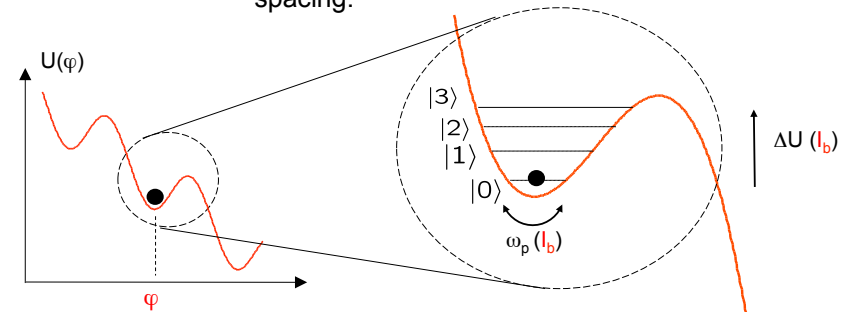


A fictitious particle trapped in a local potential minima.

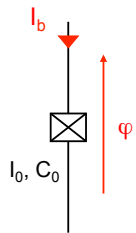
$$H = E_J \cos(\varphi) - I_b \varphi$$

Natural frequency: 
$$\omega_p = 2\pi \sqrt{\frac{E_J}{\phi_0^2 C}}$$

Discrete energy levels with distinct energy levels spacing.



## A quantum anharmonic oscillator

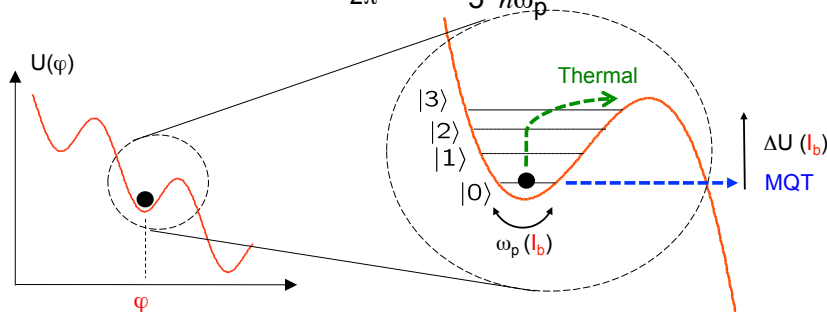


Escape is both through thermal activation by reaching a unconfined state:

$$\Gamma_{TA} = \frac{\omega_p}{2\pi} \exp\left(-\frac{\Delta U}{k_B T}\right)$$

and by Macroscopic Quantum Tunneling (MQT).

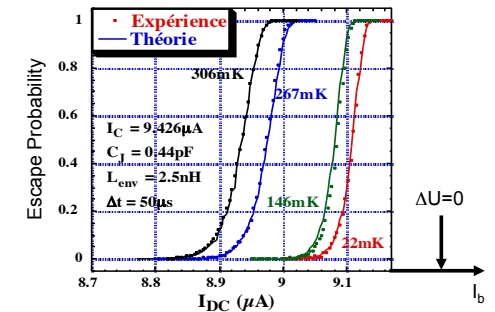
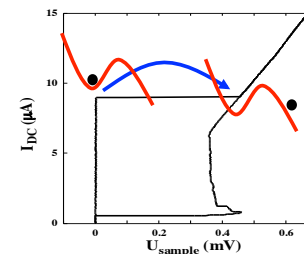
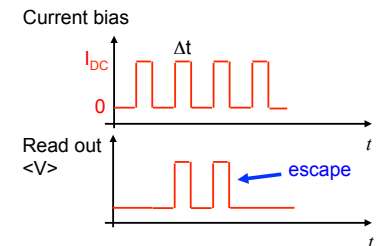
$$\Gamma_{MQT} = \frac{\omega_p}{2\pi} \exp\left(-\frac{36}{5} \frac{\Delta U}{\hbar \omega_p}\right)$$



## Escape measurements

Escape detected as the switch from zero voltage to the gap.

Stochastic process: a statistical analysis is needed.



# Macroscopic quantum tunneling

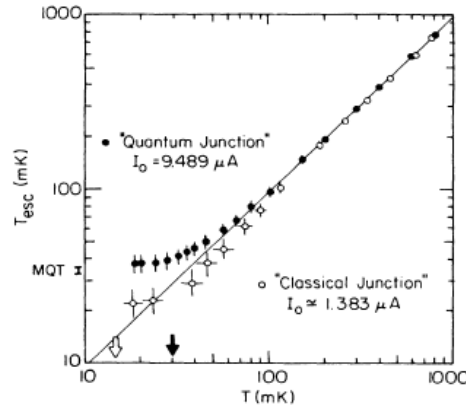
Escape rate described through an escape temperature  $T_{sc}$ :

$$\Gamma = \frac{\omega_p}{2\pi} \exp\left(-\frac{\Delta U}{k_B T_{esc}}\right)$$

Crossover between TA and MQT at:

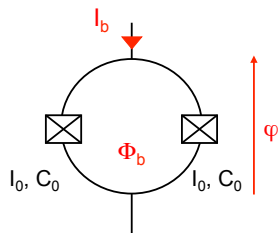
$$T \approx \frac{\hbar \omega_p}{7k_B}$$

J. M. Martinis et al, Phys. Rev. B 35, 4682 (1987).



## 3.3 A SQUID as a phase qubit

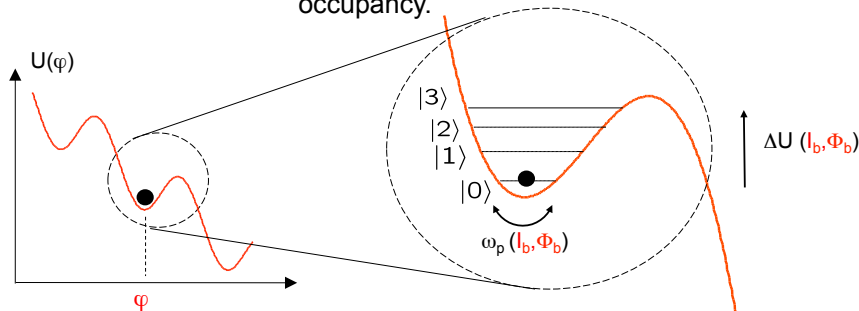
### A SQUID as a phase qubit



The two levels 0 and 1 can be the basis for a qubit.

With a SQUID geometry, the barrier width and height are controlled by the flux.

The escape measurement rate gives the state occupancy.



### Rabi oscillations (I)

Two-level system submitted to rf:

$$H = \begin{pmatrix} -\frac{1}{2}\hbar\omega_{01} & -A\cos(\omega t) \\ -A\cos(\omega t) & \frac{1}{2}\hbar\omega_{01} \end{pmatrix}$$

$\hbar\omega_{01} = E_1 - E_0$

Ansatz for the state  $|\psi(t)\rangle = C_0(t)e^{i\omega_{01}t/2}|0\rangle + C_1(t)e^{-i\omega_{01}t/2}|1\rangle$

Inserted into time-dependent Schrödinger eq.  $H\psi(z) = i\hbar \frac{d\psi}{dt}$

$$\begin{aligned} \dot{C}_0 &= \frac{i}{\hbar} A \cos(\omega t) e^{-i\omega_{01}t} C_1 \\ \dot{C}_1 &= \frac{i}{\hbar} A \cos(\omega t) e^{i\omega_{01}t} C_0 \end{aligned}$$

Rotating Wave Approximation:  
terms oscillating at  $\omega + \omega_{01}$  neglected.

$$\begin{aligned} \dot{C}_0 &= \frac{i}{2\hbar} A e^{i(\omega - \omega_{01})t} C_1 \\ \dot{C}_1 &= \frac{i}{2\hbar} A e^{-i(\omega - \omega_{01})t} C_0 \end{aligned}$$

$$\ddot{C}_1 + i(\omega - \omega_{01})\dot{C}_1 + \frac{A^2}{4\hbar^2} C_1 = 0$$



## Rabi oscillations (II)

Solutions of the type:  $C_1(t) = e^{i\lambda t}$

$$\begin{array}{c} \text{?} \\ |1\rangle \\ |0\rangle \end{array} \quad \lambda_{\pm} = \frac{1}{2} \left( \Delta \pm \sqrt{\Delta^2 + A^2} \right)$$

$$\Delta = \omega - \omega_{01}$$

General solution:  $C_1(t) = C_+ e^{i\lambda_+ t} + C_- e^{i\lambda_- t}$   
System initially in the ground state:  $C_0 = 1$ ;  $C_1 = 0$ .

$$C_0(t) = e^{-i\Delta t/2} \left( \cos(\Omega_R t/2) + i \frac{\Delta}{\Omega_R} \sin(\Omega_R t/2) \right)$$

$$\Omega_R^2 = \sqrt{\Delta^2 + A^2} / \hbar^2$$

$$C_1(t) = i \frac{A}{\Omega_R \hbar} e^{i\Delta t/2} \sin(\Omega_R t/2)$$

Probability to find the system in the excited state:

$$P_1(t) = |C_1(t)|^2 = \frac{A^2}{\Omega_R^2 \hbar^2} \sin^2(\Omega_R t/2)$$

## Rabi oscillations (III)

A rf signal at  $\hbar\omega \approx \hbar\omega_{01}$  is sent to the qubit (at ground state 0) for a duration  $t$ . The qubit arrives at the excited state 1 with a probability:

$$P_1(t) = \frac{A^2}{\Omega_R^2 \hbar^2} \sin^2(\Omega_R t/2)$$

Rabi oscillations:  
proof of quantum-coherent behavior

$$\Omega_R^2 = \sqrt{\Delta^2 + A^2} / \hbar^2$$

If no detuning:  $\Omega_R = A / \hbar$

$$P_1(t) = \sin^2(\Omega_R t/2)$$

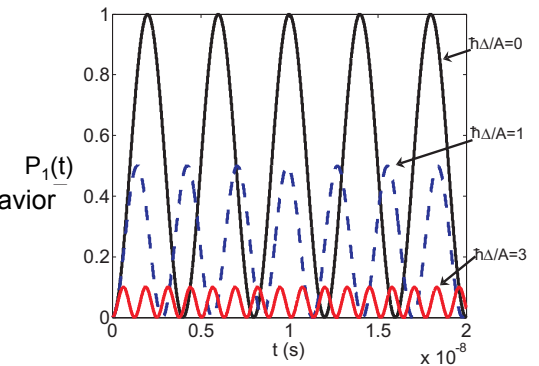
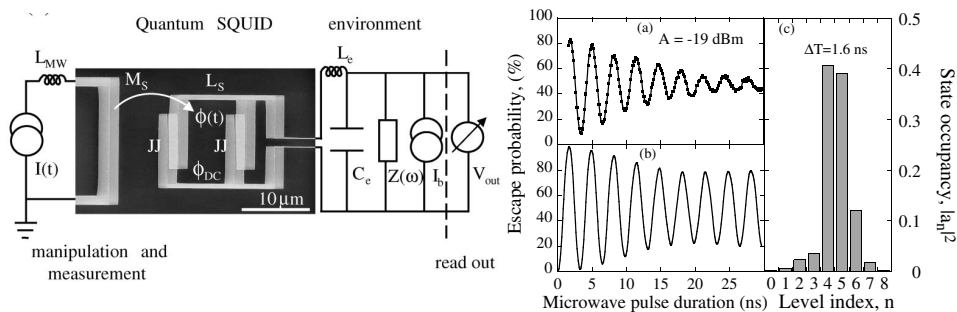


Figure 1: Rabi oscillations. Probability of finding a (two level) atom, subject to "classical" harmonic radiation, in the excited state  $|e\rangle$  as a function of time  $t$ . The transition dipole moment  $\langle e|\hat{d}|g\rangle/2\pi\hbar$  was chosen to be 250 MHz. The detuning between the harmonic radiation frequency and the atom transition frequency  $\Delta/2\pi = (\omega - \omega_0)/2\pi$  is varied between 0 MHz and 750 MHz.

## Rabi oscillations in a dc-SQUID

Decay of oscillation amplitude related to decoherence.  
At large microwave power, higher energy levels are involved.



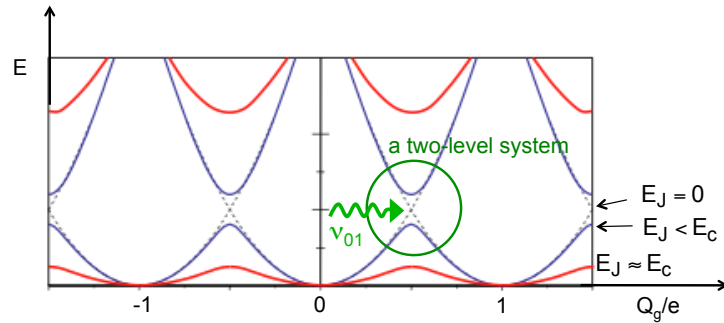
## 3.4 Josephson charge qubits

## Josephson junction in the charge regime

Considering the charge energy as a function gate voltage, the Josephson coupling opens gaps.

$$H = \frac{Q^2}{2C} + E_J \cos \varphi$$

A two-level system is thus defined.

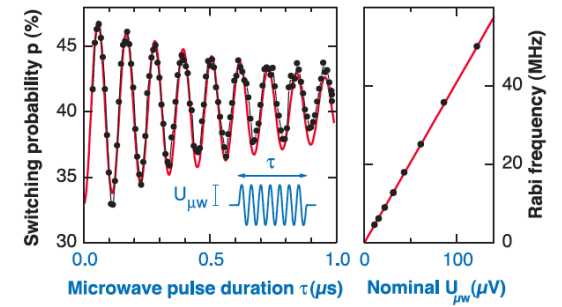
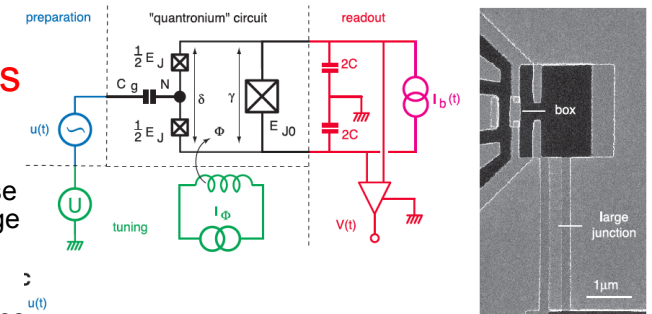


## Rabi oscillations

The state after the rf pulse can be probed with a large JJ in parallel.

Proves that the particle lies in a quantum superposition of two states.

Decay of oscillation amplitude related to decoherence.



D. Vion et al, Science 296, 886 (2002).